

1 *Title:*

2 **APPLICABILITY ASSESSMENT FOR *IN-SILICO* PATIENT-SPECIFIC TEVAR**  
3 **PROCEDURES**

4  
5 *Authors:*

6 Anna Ramella<sup>1</sup>, Francesco Migliavacca<sup>1</sup>, Jose Felix Rodriguez Matas<sup>1</sup>, Tim J. Mandigers<sup>2</sup>, Daniele  
7 Bissacco<sup>2</sup>, Maurizio Domanin<sup>2</sup>, Santi Trimarchi<sup>2</sup>, Giulia Luraghi<sup>1</sup>

8  
9 <sup>1</sup>Department of Chemistry, Materials and Chemical Engineering, Politecnico di Milano, Piazza L.  
10 da Vinci 32, 20133 Milan, Italy.

11 <sup>2</sup>Unit of Vascular Surgery, I.R.C.C.S. Fondazione Cà Granda Policlinico Milano, Via Francesco  
12 Sforza 35, Milan, Italy

13  
14 *Corresponding author:*

15 Giulia Luraghi

16 Computational Biomechanics Laboratory – LaBS

17 Department of Chemistry, Materials and Chemical Engineering ‘Giulio Natta’

18 Politecnico di Milano

19 Piazza L. da Vinci 32, 20133 Milan, Italy

20 Tel: +39.02.2399.3399

21 E-mail address: [giulia.luraghi@polimi.it](mailto:giulia.luraghi@polimi.it)

22  
23 *Keywords:*

24 stent-graft, applicability analysis, credibility, TEVAR, Finite Element

25 *Words count (Introduction to discussion):* 3486

26

27 **ABSTRACT**

28 Thoracic Endovascular Aortic Repair (TEVAR) is a minimally invasive technique to treat thoracic  
29 aorta pathologies and consists of placing a self-expandable stent-graft into the pathological region to  
30 restore the vessel lumen and recreate a more physiological condition. Exhaustive computational  
31 models, namely the finite element analysis, can be implemented to reproduce the clinical procedure.  
32 In this context, numerical models, if used for clinical applications, must be reliable and the simulation  
33 credibility should be proved to predict clinical procedure outcomes or to build *in-silico* clinical trials.  
34 This work aims first at applying a previously validated TEVAR methodology to a patient-specific  
35 case. Then, defining the TEVAR procedure performed on a patient population as the context of use,  
36 the overall applicability of the TEVAR modeling is assessed to demonstrate the reliability of the  
37 model itself following a step-by-step method based on the ASME V&V40 protocol. Validation  
38 evidence sources are identified for the specific context of use and adopted to demonstrate the  
39 applicability of the numerical procedure, thereby answering a question of interest that evaluates the  
40 deployed stent-graft configuration in the vessel.

41

42

43

44

## 45        **1. INTRODUCTION**

46        In the recent literature (Morrison et al., 2019; Pathmanathan et al., 2017; Viceconti et al., 2021) and  
47        regulatory body publications (ASME, 2018, 2006), strong emphasis is given to the role of the  
48        credibility and reliability of a computational model. Model credibility can be defined as the capability  
49        of a numerical model to address a given question of interest (QOI) or predict a specific context of use  
50        (COU), through the collection of evidence (Pathmanathan et al., 2017).

51        In 2018, the American Society of Mechanical Engineering (ASME, 2018) introduced a verification  
52        and validation (V&V) standard for medical device applications to establish the credibility needed to  
53        support the use of computational models. Verification and validation are two different aspects both  
54        responsible for gaining the accuracy and reliability of the computational results (Oberkampf et al.,  
55        2004). Verification is related to the process of determining if the computational simulation is accurate  
56        to reproduce the underlying mathematical model. Validation is the process of determining if the  
57        mathematical model is accurate in representing the real scenario. A relevant aspect of credibility  
58        assessment is the applicability analysis, defined as the use of a computational model in a specific  
59        COU supported by validation evidence. A work by Pathmanathan et al., 2017 describes twelve steps  
60        for developing the applicability analysis providing a framework for evaluating and justifying the use  
61        of an *in-silico* model for a specific COU. In the field of cardiovascular numerical models, few works  
62        addressed the applicability analysis following a rigorous framework. Luraghi et al., 2021 applied the  
63        credibility process to thrombectomy procedure simulations. Pathmanathan and Gray, 2018  
64        demonstrated the trustworthiness of multiscale models of cardiac electrophysiology. Santiago et al.,  
65        2022 assessed the model credibility flow distortion introduced in the left ventricle by the left  
66        ventricular assist devices. In Morrison et al., 2019, the credibility assessment framework was applied  
67        to haemolysis in centrifugal blood pumps.

68        The proposed study focuses on the Thoracic Endovascular Aortic Repair (TEVAR) procedure, a  
69        minimally invasive technique for treating aortic pathologies in which a self-expandable stent-graft is  
70        inserted and deployed in the pathological region to treat the patient and recreate a more physiological

71 situation (Findeiss and Cody, 2011). The numerical model able to simulate the stent-graft deployment  
72 and its interaction with the aortic wall has already been discussed and validated in a previous study  
73 of ours (Ramella et al., 2022). This work aims at: (1) presenting and discussing the first patient-  
74 specific pilot study based on the validated virtual TEVAR procedure (Ramella et al., 2022); (2)  
75 providing an applicability assessment for patient-specific TEVAR procedures following the  
76 framework proposed by Pathmanathan et al., 2017.

## 77 **2. PILOT PATIENT-SPECIFIC *IN-SILICO* TEVAR CASE**

### 78 **2.1. Materials and methods**

79 *Clinical patient data.* The selected patient was a 63-years-old man, with his first hospital  
80 admission due to an asymptomatic Penetrating Aortic Ulceration (PAU) located in his left hemi-aortic  
81 arch. The patient had a bovine aortic arch with a common origin of the brachiocephalic trunk and left  
82 common carotid artery (LCCA). Diameters of the PAU measured 26 by 32 mm in axial and sagittal  
83 sections. TEVAR was performed at the Fondazione IRCCS Cà Granda Ospedale Maggiore  
84 Policlinico, Milan, Italy. The proximal landing zone was directly distal to the bovine supra-aortic  
85 trunk (zone 2) and a 34x34x100 proximal free-flo Valiant Captivia® stent graft (Medtronic, Inc.,  
86 MN, U.S.A.) was implanted. A 2-month control postoperative CTA (Computed Tomography  
87 Angiography) confirmed the thoracic aortic endograft's correct position without complications.  
88 Informed consent regarding the specific treatment and data usage was signed by the patient. Approval  
89 for this specific study was waived by the local ethical committee.

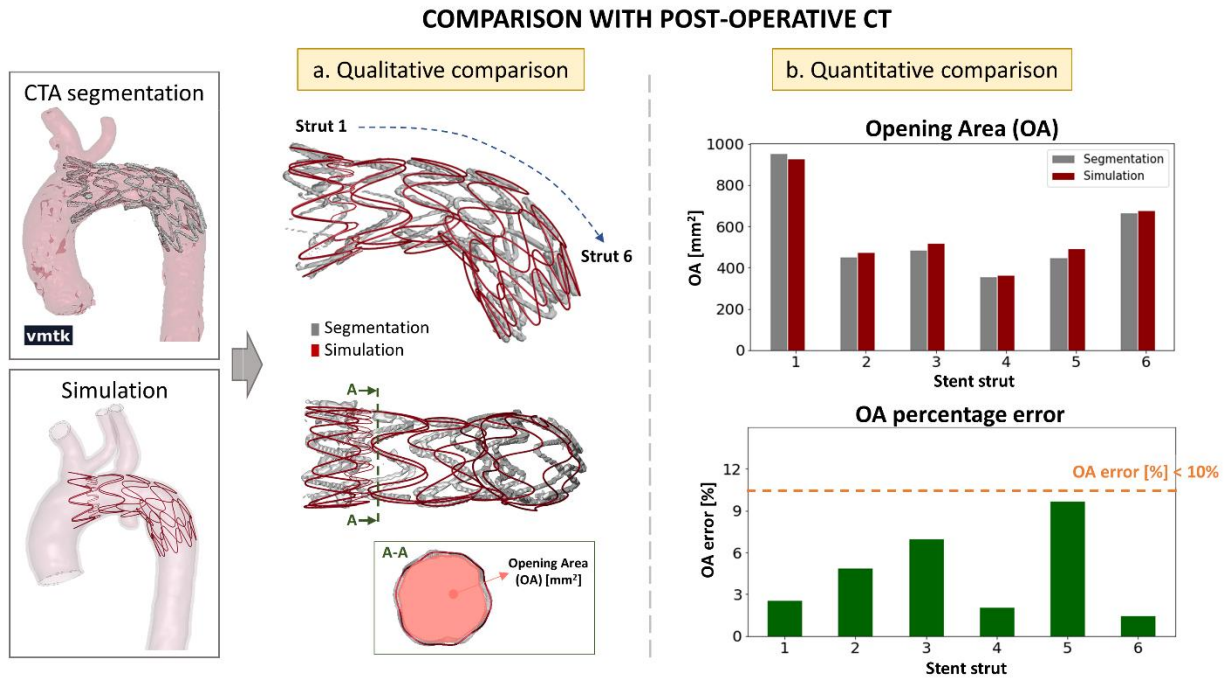
90 *Numerical models.* The 34x34x100 Valiant Captivia (Medtronic, Inc., MN, U.S.A.) stent-graft  
91 was modeled following Ramella et al., 2022 (Figure 1.a). The stent was discretized with beam  
92 elements (1232 elements with an average size of 1 mm) and the graft with triangular membrane  
93 elements (16414 elements with an average size of 1 mm). Nitinol shape memory material formulation  
94 for the stent and a fabric material formulation for the graft were adopted. Material parameters can be  
95 found in Ramella et al., 2022.

96 The pre-operative patient-specific aorta lumen was segmented from CTA images using the software  
97 VMTK (Orobix s.r.l.) and a constant 1.8 mm of thickness was extruded to create the aorta wall  
98 (Choudhury et al., 2009). It was discretized with tetrahedral elements (423891 elements with an  
99 average size of 0.75 mm) with three layers of elements through the vessel wall thickness (Figure 1.b).  
100 The aorta material was modeled with an isotropic hyperelastic law following the Yeoh constitutive  
101 formulation with literature material parameters (Simsek and Kwon, 2015).  
102 The TEVAR simulation follows the steps discussed in our previous work (Ramella et al., 2022).  
103 Briefly, the device, which is in a pre-stressed state was crimped and displaced inside the aorta  
104 (tracking phase) until the proximal landing zone was reached and then gradually deployed (Figure  
105 1.c). More details on the simulation set-up and vessel geometry post-process can be found in the  
106 Supplementary material.  
107 To validate the simulation result, the stent deployed configuration obtained with the simulation was  
108 qualitatively and quantitatively compared with the stent configuration reconstructed from the post-  
109 operative CTA images of the patient, following the framework proposed in Ramella et al., 2022  
110 (Figure 2). The stent was segmented using the software VMTK (Orobix srl.).

111

## 112 **2.2. Results**

113 Some of the structural results of the TEVAR simulations are reported in Figure 1.d. The distance  
114 between the stent-graft and aorta and Von Mises stress distribution on the aortic wall at the end of  
115 deployment are depicted. The struts are mostly in contact with the aortic wall, with the exception of  
116 the peaks of the proximal free flow ring due to the vessel anatomy, which presents a low radius of  
117 curvature. The anatomy features influence also the von Mises stress distribution: the stress values are  
118 maximum in the central region of the stent at the level of the internal aortic curvature and decrease  
119 towards the proximal sections.



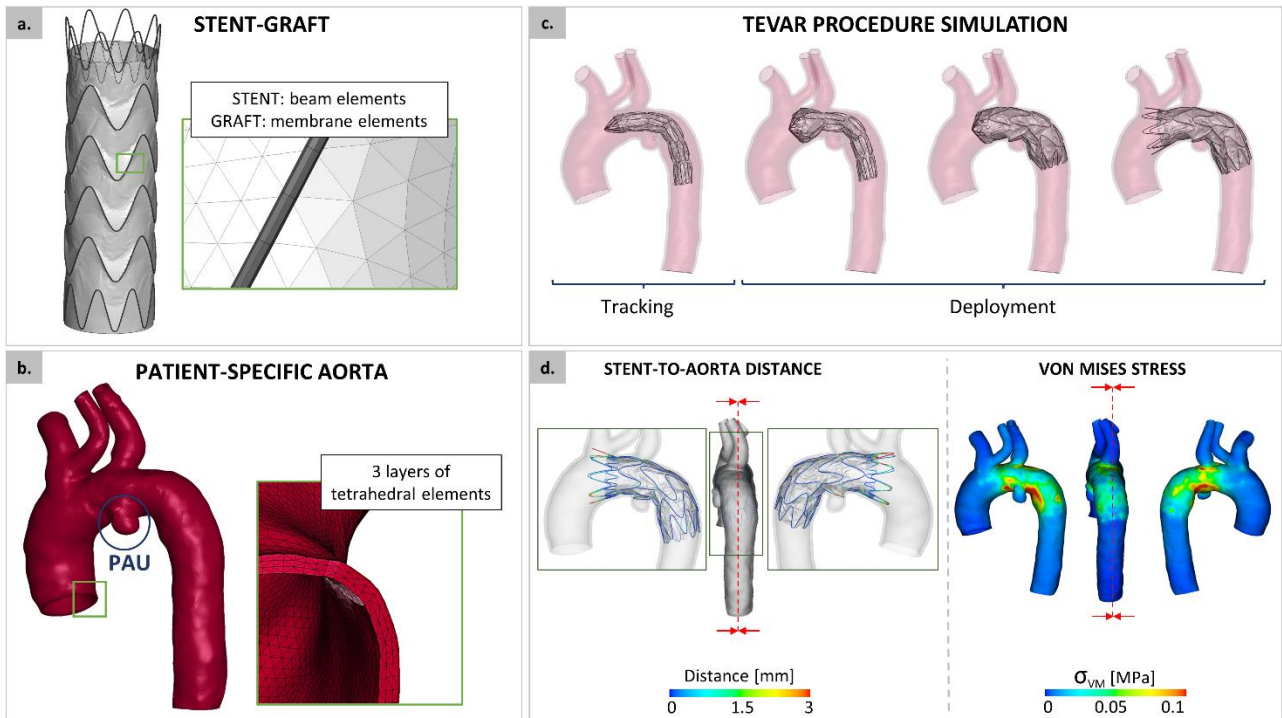
120

121 **Figure 1.** (a.) Finite Element 34x34x100 Valiant Captivia stent-graft model with mesh details. (b.)  
 122 The patient-specific aortic model with mesh details. (c.) Tracking and deployment steps of the  
 123 TEVAR simulation. (d.) Simulation results evaluated at the end of stent-graft deployment: distance  
 124 between the stent struts and the aortic wall (left) and von Mises stress distribution on the aortic wall  
 125 (right).

126

127

128 In Figure 2, the comparison between the simulation and post-operative CTA stent segmentation is  
 129 also reported and a good overlap is achieved between the simulated and segmented stent  
 130 configurations. By evaluating the opening area for each stent strut, the errors between the simulation  
 131 and CTA reconstruction are below 10%.



132

133

134

135

136

137

### 3. APPLICABILITY ANALYSIS

138

139

140

141

142

**Figure 2.** Assessment of stent-graft deployed configuration between the simulation results and CTA segmentation: (a.) Qualitative overlap and example of Opening Area (OA) estimation for a stent strut; (b.) quantitative comparison of the OA for each stent strut and calculation of percentage errors.

The second aim of this work is to discuss and justify the applicability and credibility of patient-specific TEVAR simulation of stent-graft implantation, following the process described in Pathmanathan et al., 2017: three main steps are here proposed as reported in Table 1.

**Table 1.** Steps of the applicability analysis.

Steps of the applicability analysis	
<b>Step 1.</b>	Description of the real environmental settings and corresponding computational models.
<b>Step 2.</b>	Lists of the equalities and differences between the validation and COU models and reality.

<b>Step 3.</b>	Discussion of the applicability assessment.
----------------	---

143

144

145

146 **3.1. Step 1. Description of the real environmental settings and corresponding computational**  
147 **models.**

148 The main purpose of the computational TEVAR modeling is to replicate the clinical procedure  
149 performed with stent-graft models in virtual patients. The computational process can be used to  
150 predict the stent-graft deployed configuration after the TEVAR procedure in a virtual population,  
151 answering a specific question of interest (QOI). The herewith QOI is “Will a given stent-graft model  
152 be successfully deployed in a given patient-specific aorta in a given position with respect to the  
153 location of the pathology (e.g., aneurysm, dissection, PAU)?”. From a clinical point of view, the stent-  
154 graft is successfully deployed if it is completely apposed to the aortic wall at the proximal and distal  
155 landing zones (Nation and Wang, 2015). From an engineering perspective, the deployment can be  
156 quantitatively evaluated by measuring the distance between the stent-graft and the aorta in relevant  
157 regions.

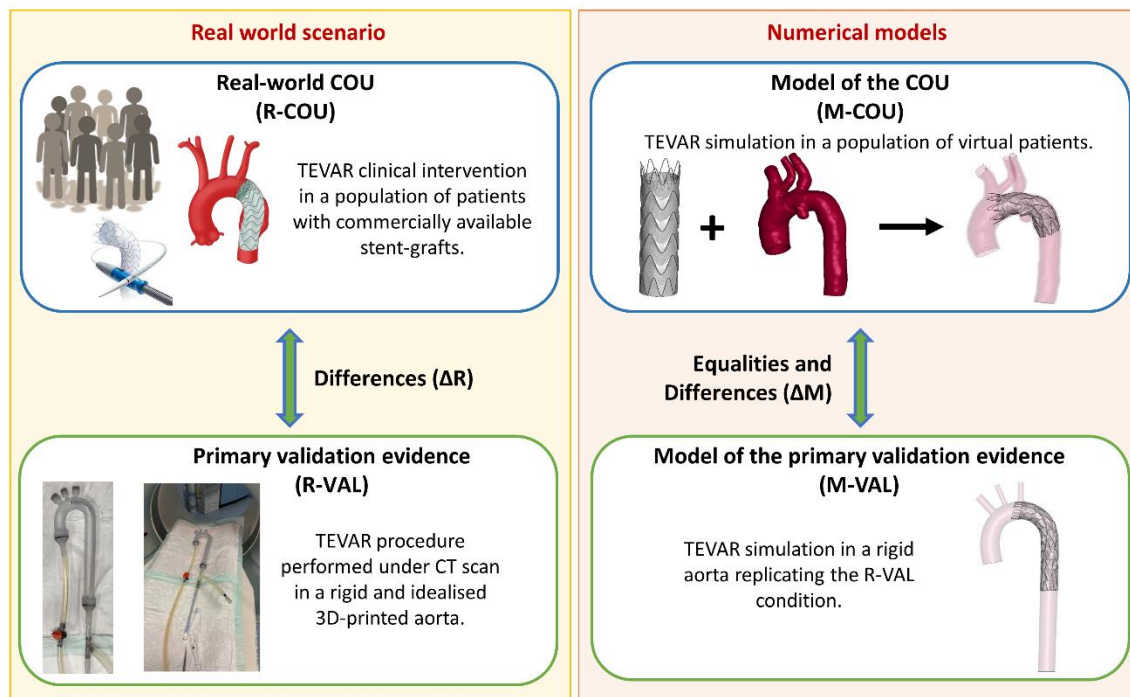
158

159 In this analysis, two frameworks (Figure 3) are outlined: the COU and the validation evidence (VAL).  
160 Among them, the real-world scenario (R-COU and R-VAL) and the numerical models (M-COU and  
161 M-VAL) are identified. The model elements of the context of use (M-) represent the computational  
162 models used to replicate the real-world setting scenarios (R-).

163 In this work, the **R-COU** is related to the clinical TEVAR procedure performed on patients with  
164 different pathologies, and with different commercially available stent-grafts, requiring different  
165 deployment procedures. On the other hand, the **M-COU** comprises the finite element (FE) models of



166 the commercial stent-graft and the patient-specific aorta to virtually reproduce the clinical procedure,  
 167 as shown in the pilot study of the previous paragraph.  
 168



169  
 170 **Figure 3.** On the left, the real-world scenario of the context of use and validation evidence: the real  
 171 environment setting (R-COU) and the physical primary validation evidence (R-VAL). On the right,  
 172 numerical models of the context of use and validation evidence: the COU model adopted to address  
 173 the QOI (M-COU) and the primary validation computational model (M-VAL).

174  
 175 The adoption of a computational model for predicting the real scenario must be supported by a series  
 176 of validation results. The following validation evidence sources are available, all of them deeply  
 177 discussed in Ramella et al., 2022:

- 178 1) *Validation of the Nitinol material.* Crimping/release experimental tests on Valiant Captivia  
 179 stent struts are performed to calibrate and validate the Nitinol material parameters.  
 180 2) *Validation of the stent-graft model.* Crimping/release experimental tests on two Valiant  
 181 Captivia stent-grafts are used to validate the stent-graft models.

182 3) *Validation of the TEVAR procedure in an idealised rigid aorta.* A rigid 3D-printed idealized  
183 aorta is used to experimentally implant a stent-graft under a CT (Computed Tomography)  
184 scan. The stent configuration obtained with the experiment is adopted to validate the  
185 simulation results.

186 The validation evidence (3) is considered as the primary validation evidence (VAL) since it involves  
187 relevant aspects of the COU.

188 In this context, **R-VAL** and **M-VAL** refer to the real experimental and computational models of the  
189 validation evidence replicating *in-vitro* and *in-silico* the TEVAR procedure in an idealized aorta.  
190 Briefly, in R-VAL, a Valiant Captivia (Medtronic, Inc., MN, U.S.A.) stent-graft is experimentally  
191 released into a 3D-printed rigid idealized aorta and inspected in a computed tomography scan at  
192 different time points during deployment. The same stent-graft and aorta are modeled for the M-VAL  
193 numerical simulation in which the TEVAR procedure steps are replicated. Complete details about the  
194 validation evidence are reported in Ramella et al., 2022.

195

### 196 **3.2. Step 2. Lists of the equalities and differences between the VAL and COU models and** 197 **reality.**

198 The identical model aspects in the M-COU and M-VAL are:

- 199 a) Stent and graft element formulation. Given a stent-graft model, the stent is discretized with  
200 beam elements and the graft with triangular membrane elements. Also, the characteristic  
201 dimension of the elements is the same in each model.
- 202 b) Material constitutive formulation of the stent-graft. The same shape memory alloy and fabric  
203 material formulations are used for all the considered stent-graft.
- 204 c) Steps of the TEVAR simulation and software. For each stent-graft, the TEVAR simulation is  
205 composed of the same steps (crimping, tracking, deployment). The numerical details  
206 (damping and contact friction coefficients, time-step, contact algorithm), explicit solver and

207 memory requirements (28 CPU and 250 GB of RAM memory) of the simulations are the  
208 same.

209 d) QOIs. In both M-VAL and M-COU, the QOI is related to the estimation of the deployed stent-  
210 graft configuration.

211

212 On the other hand, the following model aspects are different in the M-COU and M-VAL ( $\Delta M$ ).

213 a) Aorta geometry. In the M-COU, a patient-specific aorta is involved, while an idealized aorta  
214 is used in M-VAL.

215 b) Aorta element formulation and material properties. In the M-COU tetrahedral elements are  
216 used and a deformable hyperelastic material is assigned to the aortic wall, while rigid shell  
217 elements are adopted in M-VAL.

218 c) Stent-graft model, size and materials. In the M-VAL a Valiant Captivia stent-graft  
219 (34x34x200 mm size) is implanted with calibrated material parameters. In M-COU, each  
220 commercially available stent-graft model and size can be adopted and modelled with its  
221 specific material properties. Single parameters of the material modes used in each stent-graft  
222 can differ after proper calibration analysis.

223 d) Position of the stent-graft into the aorta. In M-VAL the stent-graft position reflects the  
224 experimental one of R-VAL, in M-COU it can vary depending on the patient's anatomy.

225

226 The following model aspects are different in the R-COU and R-VAL ( $\Delta R$ ).

227 a) Aorta geometry and material. In the R-VAL, the idealized aortic model is realized with  
228 physiological dimensions and 3D printed with a rigid transparent isotropic material (Stratasys  
229 VeroClear RGD810) with a thickness of 1.5 mm (more details in the Supplementary material).  
230 In the R-COU, aortic dimensions, pathologies and material properties (nonlinear, anisotropic,  
231 presence of thrombi or calcifications) change among patients.

- 232 b) Stent-graft model. In the R-COU, TEVAR can be performed with any commercially available  
233 stent-graft. In the R-VAL, a Valiant Captivia stent-graft (34x34x200 mm size) is used.
- 234 c) TEVAR procedure. In the R-COU the device location is strictly related to the location of the  
235 pathology while an optimal stent-graft positioning is chosen in the R-VAL experiments. In  
236 the R-COU the stent-graft is inserted from the femoral artery, in the R-VAL the aortic model  
237 is shorter (up to the renal arteries bifurcation).
- 238 d) Blood flow. The R-VAL is performed with stationary water at 37°C, while in the R-COU  
239 blood is continuously flowing creating a dynamic environment.

240

### 241 **3.3. Step 3. Discussion on the applicability assessment.**

242 In this paragraph, the equalities and differences listed above are deeper discussed and justified to  
243 demonstrate the overall applicability of the TEVAR model. The key point of the applicability  
244 appraisal is the analysis of these identical/dissimilar aspects by answering the question: “*since we*  
245 *assume that it is appropriate to model the R-VAL with the validation results (M-VAL), is it*  
246 *appropriate to use a specific model (M-COU) to predict the R-COU given the differences between R-*  
247 *VAL and R-COU?*”.

248 First, the identical aspects between M-VAL and M-COU are discussed in light of the differences  $\Delta R$   
249 of the real settings (Table 2).

250

251

252

253

254

255

256

257 **Table 2.** Identical aspects between M-VAL and M-COU in light of the differences between the R-  
 258 VAL and R-COU.

Differences between R-VAL and R-COU ( $\Delta R$ )	Identical aspects between M-VAL and M-COU			
	Stent and graft materials	Element formulations	Steps of the simulation	QOIs
a) Aorta geometry and material properties.			<sup>(3)</sup> Are the simulation steps suitable for modeling the TEVAR procedure of the R-COU?	
b) Stent-graft model.	<sup>(1)</sup> Are the stent- graft materials applicable to any stent-graft in the R-COU?	<sup>(2)</sup> Are the element formulations acceptable to model the TEVAR procedure of the R-COU?		
c) TEVAR procedure.				
d) Blood flow.				<sup>(4)</sup> Does the presence of the fluid affect the QOI?

259

260

261 *1) Are the stent-graft materials applicable to any stent-graft in the R-COU?* The  
 262 crimping/release tests in the R-VAL are performed with two Valiant Captivia stent-grafts sizes and  
 263 the material properties are found to be the same for both devices (supporting validation evidence 1  
 264 and 2). For this reason, we considered the stent-grafts with the same material properties independently  
 265 of the sizes (length and diameter). The same rationale stands for other commercial stent-grafts.

266           2) *Are the element formulations acceptable to model the TEVAR procedure of the R-COU?*

267 For the same reasons discussed above, all the stent-grafts are discretized in the same way. Modelling  
268 the stent with beam elements has been demonstrated (Ramella et al., 2022) to be suitable for correctly  
269 describing the stent kinematics during deployment and answering the QOI.

270           3) *Are the simulation steps suitable for modeling the TEVAR procedure of the R-COU?* The  
271 steps of the simulations (crimping, tracking, deployment) reflect the real TEVAR of R-COU as well  
272 as the replication of the experimental procedure of R-VAL. In the simulation, the stent-graft is  
273 displaced along the vessel centerline. Differently, in the real scenario, a guidewire is inserted  
274 deviating the device trajectory from the centerline. However, this difference is supported by the  
275 primary validation evidence. In the R-COU, access to the patient is performed from the femoral  
276 artery, while in the R-VAL, a shorter aortic model is considered. This does not affect the results since,  
277 in both cases, the stent-graft remained crimped within the catheter until the proximal landing zone is  
278 reached. The simulation steps are also tailored to the stent-graft size (e.g., a longer device means  
279 higher tracking phase time)

280           4) *Does the presence of the fluid affect the QOI?* The main aim of the models is on the stent-  
281 graft and aorta interactions, and therefore FE simulations are carried out neglecting the presence of  
282 the fluid. The R-VAL is performed under stationary flow water at 37°C. The steadiness of the flow  
283 allows the simplification of the model to structural simulation instead of fluid-structure interaction  
284 simulation. Since the simulation was validated without modeling blood flow (supporting validation  
285 evidence 3.), the stent-graft patient-specific implantation can be performed without fluid as well: as  
286 shown in the pilot study, the simulation leads to a reliable deployed stent-graft configuration.

287  
288 In the light of this analysis, the differences  $\Delta M$  between M-VAL and M-COU are described to discuss  
289 whether modifications of the computational model result in trustworthy predictions for the COU.

290           a) Vessel geometry. In the M-VAL the aorta is idealized: the goal of the primary validation is to  
291 trustily replicate the TEVAR deployment. In the M-COU the patient-specific aorta is

292 segmented from CTA images. Patient-specific anatomy does not affect the trustworthy  
293 prediction of the M-COU as demonstrated by the presented pilot patient-specific analysis.  
294 Nevertheless, a change in the vessel anatomy leads to changes in pathology, curvature, and  
295 tortuosity which, from the clinical point of view, are factors that affect the outcome of the  
296 TEVAR procedure (Findeiss and Cody, 2011; Marrocco-Trischitta et al., 2018; Nation and  
297 Wang, 2015; Sweet, 2016; Ueda et al., 2011).

298 b) Aorta element formulation and material properties. In the M-COU tetrahedral elements are  
299 used, while shell elements are adopted in the M-VAL. In the M-VAL the aorta is rigid, thus  
300 modeling the vessel with shells or solid elements does not significantly affect the results (shell  
301 elements are chosen to reduce the computational time). This material simplification (rigid  
302 instead of deformable) was chosen since the M-VAL focused on the device deployment,  
303 removing uncertainties related to the aortic wall materials. Differently, the M-COU aortic  
304 wall is modeled with a hyperelastic isotropic material to introduce the aortic wall deformations  
305 during deployment. The differences between M-COU and M-VAL are overcome given the  
306 results obtained with the pilot patient-specific application. In fact, the simulated stent  
307 configuration showed a good prediction of reality when compared to the post-operative CTA  
308 stent reconstruction (Figure 2).

309 c) Stent-graft model, size, and materials. In the M-VAL a Valiant Captivia stent-graft  
310 (34x34x200 mm size) is implanted with calibrated material parameters. The virtual TEVAR  
311 of the M-COU can be performed with any commercial stent-graft. In particular, all the stent-  
312 grafts are modeled with the same discretization technique and with material parameters  
313 calibrated with the same protocols (supporting validation evidence). Differences in device  
314 size are taken into account in the steps of the TEVAR procedure simulation.

315 d) Position of the stent-graft into the aorta. In M-VAL the stent-graft position reflects the  
316 experimental one of R-VAL, in M-COU it can vary depending on the patient's anatomy. The  
317 position of the pathology only affects the TEVAR simulation. The ability of the model to

318 consider these changes is proven by the pilot study which considers patient-specific anatomy  
319 instead of an idealized one.

320

#### 321 **4. DISCUSSION**

322 The model credibility is related to the capability of the model to adequately reproduce an identified  
323 context of use and it is of foremost importance if the model will be used for clinical applications.  
324 Activities such as verification, validation and evaluation of the applicability of the numerical model  
325 must be considered, to establish how reliable the model is, as suggested by the V&V 40 standard  
326 introduced by the American Society of Mechanical Engineering (ASME, 2018). In particular, the  
327 assessment of the *in-silico* model applicability is a fundamental aspect to demonstrate the reliability  
328 of the model itself in a specified COU, as described in the step-by-step framework proposed by  
329 Pathmanathan et al., 2017. Among the literature, some studies carried out an exhaustive applicability  
330 analysis of the numerical model in different cardiovascular fields such as thrombectomy (Luraghi et  
331 al., 2021), cardiac electrophysiology (Pathmanathan and Gray, 2018), left ventricle blood flow after  
332 LVAD (Santiago et al., 2022) or haemolysis (Morrison et al., 2019). To the best of the authors'  
333 knowledge, this is the first study that investigates the applicability of the TEVAR numerical  
334 modeling, following the framework proposed by Pathmanathan et al., 2017.

335 In this work, the finite element-based TEVAR procedure previously developed (Ramella et al., 2022)  
336 is successfully applied to a patient-specific aorta. Comprehensively, the numerical workflow starts  
337 with the segmentation of the patient-specific aortic model from pre-operative CTA images, followed  
338 by its finite element discretization. Then, once the commercial stent-graft size is selected and  
339 discretized, the simulation of the TEVAR procedure is performed. The presented pilot study is a  
340 fundamental step in gaining the reliability of the overall TEVAR computational model and it helps  
341 in contextualizing the following applicability analysis of the *in-silico* modeling. Although it has some  
342 limitations and could be further improved (e.g., the addition of vessel pre-stress, the inclusion of the



343 blood, the exact position of the guide-wire), it demonstrates the capability to apply a validated  
344 methodology to patient-specific anatomies, that could be used to predict clinical outcomes in the  
345 future. In fact, with respect to the QOI, the most relevant simulation result is to obtain a reliable stent-  
346 graft deployed configuration. In the pilot study, this is proved by the comparison of the simulation  
347 result with the post-operative CTA of the patient: in the final deployed configuration, the error  
348 between the segmented stent and simulated one is below 10%, coherent with other literature studies  
349 (Kan et al., 2021b, 2021a; Perrin et al., 2015). The applicability of this *in-silico* model is assessed by  
350 analysing and arguing equalities and differences between the COU (TEVAR procedure in a patient  
351 population) and the validation evidence between the real-world settings and the models.  
352 In conclusion, the discussed applicability analysis demonstrated that the developed *in-silico* model is  
353 trustworthy for replicating the TEVAR procedure in virtual patients. In particular, the pilot study  
354 reports the application of TEVAR to a single patient with one specific commercial stent-graft. A  
355 population of aortic anatomies with different pathologies treated with any commercially available  
356 device could be embraced in the future, towards an *in-silico* clinical trial.

357

### 358 ***Conflict of interest statement***

359 Santi Trimarchi is a speaker and consultant for W.L. Gore & Associates, Terumo Aortic, and  
360 Medtronic Incorporated.

361 The other authors declare that they have no conflict of interest.

### 362 ***Acknowledgement***

363 This study has received funding from the MIUR FISR-FISR2019\_03221 CECOMES.

364

### 365 ***References***

366 ASME, 2018. V&V40 - 2018 - Assessing credibility of computational modeling through

- 367 verification and validation: application to medical devices. *Asme V&V* 40-2018 60.
- 368 ASME, 2006. *Guide for Verification and Validation in Computational Solid Mechanics*. Am. Soc.  
369 Mech. Eng. 1–53.
- 370 Choudhury, N., Bouchot, O., Rouleau, L., Tremblay, D., Cartier, R., Butany, J., Mongrain, R.,  
371 Leask, R.L., 2009. Local mechanical and structural properties of healthy and diseased human  
372 ascending aorta tissue. *Cardiovasc. Pathol.* 18, 83–91.  
373 <https://doi.org/10.1016/J.CARPATH.2008.01.001>
- 374 Findeiss, L.K., Cody, M.E., 2011. Endovascular Repair of Thoracic Aortic Aneurysms. *Semin.*  
375 *Intervent. Radiol.* 28, 107. <https://doi.org/10.1055/S-0031-1273945>
- 376 Kan, X., Ma, T., Dong, Z., Xu, X.Y., 2021a. Patient-Specific Virtual Stent-Graft Deployment for  
377 Type B Aortic Dissection: A Pilot Study of the Impact of Stent-Graft Length. *Front. Physiol.*  
378 12, 1171. <https://doi.org/10.3389/FPHYS.2021.718140/BIBTEX>
- 379 Kan, X., Ma, T., Lin, J., Wang, L., Dong, Z., Xu, X.Y., 2021b. Patient-specific simulation of stent-  
380 graft deployment in type B aortic dissection: model development and validation. *Biomech.*  
381 *Model. Mechanobiol.* 20, 2247–2258. [https://doi.org/10.1007/S10237-021-01504-](https://doi.org/10.1007/S10237-021-01504-X/TABLES/4)  
382 [X/TABLES/4](https://doi.org/10.1007/S10237-021-01504-X/TABLES/4)
- 383 Luraghi, G., Bridio, S., Miller, C., Hoekstra, A., Rodriguez Matas, J.F., Migliavacca, F., 2021.  
384 Applicability analysis to evaluate credibility of an in silico thrombectomy procedure. *J.*  
385 *Biomech.* 126, 110631. <https://doi.org/10.1016/J.JBIOMECH.2021.110631>
- 386 Mandigers, J. tim, Bissacco, D., Domanin, M., Piffaretti, G., Herwaarden, J.A. Van, Trimarchi, S.,  
387 2021. Complications and Failure Modes in the Proximal Thoracic Aorta. *Endovasc. Today* 20.
- 388 Marrocco-Trischitta, M.M., van Bakel, T.M., Romarowski, R.M., de Beaufort, H.W., Conti, M.,  
389 van Herwaarden, J.A., Moll, F.L., Auricchio, F., Trimarchi, S., 2018. The Modified Arch

- 390 Landing Areas Nomenclature (MALAN) Improves Prediction of Stent Graft Displacement  
391 Forces: Proof of Concept by Computational Fluid Dynamics Modelling. *Eur. J. Vasc.*  
392 *Endovasc. Surg.* 55, 584–592. <https://doi.org/10.1016/j.ejvs.2017.12.019>
- 393 Morrison, T.M., Hariharan, P., Funkhouser, C.M., Afshari, P., Goodin, M., Horner, M., 2019.  
394 Assessing Computational Model Credibility Using a Risk-Based Framework: Application to  
395 Hemolysis in Centrifugal Blood Pumps. *ASAIO J.* 65, 349–360.  
396 <https://doi.org/10.1097/MAT.0000000000000996>
- 397 Nation, D.A., Wang, G.J., 2015. TEVAR: Endovascular Repair of the Thoracic Aorta. *Semin.*  
398 *Intervent. Radiol.* 32, 265–271. <https://doi.org/10.1055/S-0035-1558824/ID/JR00904A-38>
- 399 Oberkampf, W.L., Trucano, T.G., Hirsch, C., 2004. Verification, validation, and predictive  
400 capability in computational engineering and physics. *Appl. Mech. Rev.* 57, 345–384.  
401 <https://doi.org/10.1115/1.1767847>
- 402 Pathmanathan, P., Gray, R.A., 2018. Validation and trustworthiness of multiscale models of cardiac  
403 electrophysiology. *Front. Physiol.* 9, 106.  
404 <https://doi.org/10.3389/FPHYS.2018.00106/BIBTEX>
- 405 Pathmanathan, P., Gray, R.A., Romero, V.J., Morrison, T.M., 2017. Applicability Analysis of  
406 Validation Evidence for Biomedical Computational Models. *J. Verif. Valid. Uncertain.*  
407 *Quantif.* 2. <https://doi.org/10.1115/1.4037671>
- 408 Perrin, D., Badel, P., Orgéas, L., Geindreau, C., Dumenil, A., Albertini, J.N., Avril, S., 2015.  
409 Patient-specific numerical simulation of stent-graft deployment: Validation on three clinical  
410 cases. *J. Biomech.* 48, 1868–1875. <https://doi.org/10.1016/J.JBIOMECH.2015.04.031>
- 411 Ramella, A., Migliavacca, F., Felix, J., Matas, R., Heim, F., Dedola, F., Marconi, S., Conti, M.,  
412 Allievi, S., Mandigers, T.J., Bissacco, D., Domanin, M., Trimarchi, S., Luraghi, G., 2022.

- 413 Validation and Verification of High-Fidelity Simulations of Thoracic Stent-Graft Implantation.  
414 *Ann. Biomed. Eng.* 2022 1–13. <https://doi.org/10.1007/S10439-022-03014-Y>
- 415 Santiago, A., Butakoff, C., Eguzkitza, B., Gray, R.A., May-Newman, K., Pathmanathan, P., Vu, V.,  
416 Vázquez, M., 2022. Design and execution of a verification, validation, and uncertainty  
417 quantification plan for a numerical model of left ventricular flow after LVAD implantation.  
418 *PLOS Comput. Biol.* 18, e1010141. <https://doi.org/10.1371/JOURNAL.PCBI.1010141>
- 419 Simsek, F.G., Kwon, Y.W., 2015. Investigation of material modeling in fluid-structure interaction  
420 analysis of an idealized three-layered abdominal aorta: aneurysm initiation and fully developed  
421 aneurysms. *J. Biol. Phys.* 41, 173–201. <https://doi.org/10.1007/S10867-014-9372-X>
- 422 Sweet, M.P., 2016. Anatomic features of the distal aortic arch that influence endovascular aneurysm  
423 repair. *J. Vasc. Surg.* 64, 891–895. <https://doi.org/10.1016/J.JVS.2016.03.424>
- 424 Ueda, T., Takaoka, H., Raman, B., Rosenberg, J., Rubin, G.D., 2011. Impact of quantitatively  
425 determined native thoracic aortic tortuosity on endoleak development after thoracic  
426 endovascular aortic repair. *AJR. Am. J. Roentgenol.* 197. <https://doi.org/10.2214/AJR.11.6819>
- 427 Viceconti, M., Pappalardo, F., Rodriguez, B., Horner, M., Bischoff, J., Musuamba Tshinanu, F.,  
428 2021. In silico trials: Verification, validation and uncertainty quantification of predictive  
429 models used in the regulatory evaluation of biomedical products. *Methods* 185, 120–127.  
430 <https://doi.org/10.1016/J.YMETH.2020.01.011>

431

432